

This is a pre print version of the following article:

Progress in melanoma modeling in vitro / Marconi, Alessandra; Quadri, Marika; Saltari, Annalisa; Pincelli, Carlo. - In: EXPERIMENTAL DERMATOLOGY. - ISSN 0906-6705. - 27:5(2018), pp. 578-586.  
[10.1111/exd.13670]

*Terms of use:*

The terms and conditions for the reuse of this version of the manuscript are specified in the publishing policy. For all terms of use and more information see the publisher's website.

20/04/2024 11:45

(Article begins on next page)

## Progress in melanoma modeling in vitro

Journal:	<i>Experimental Dermatology</i>
Manuscript ID	EXD-18-0147.R1
Manuscript Type:	Review Article
Date Submitted by the Author:	n/a
Complete List of Authors:	Marconi, Alessandra; University of Modena and Reggio Emilia, Surgical, Medical, Dental and Morphological Sciences Quadri, Marika; University of Modena and Reggio Emilia, Surgical, Medical, Dental and Morphological Sciences Saltari, Annalisa; University of Modena and Reggio Emilia, Dermatology Pincelli, Carlo; University of Modena and Reggio Emilia, Dermatology;
Keywords:	melanoma, 3D models, Spheroids, Skin equivalents, skin-on-a-chip

1  
2  
3  
4  
5  
6  
7  
8  
9  
10  
11  
12  
13  
14  
15  
16  
17  
18  
19  
20  
21  
22  
23  
24  
25  
26  
27  
28  
29  
30  
31  
32  
33  
34  
35  
36  
37  
38  
39  
40  
41  
42  
43  
44  
45  
46  
47  
48  
49  
50  
51  
52  
53  
54  
55  
56  
57  
58  
59  
60

1

## Progress in melanoma modeling in vitro

Alessandra Marconi, Marika Quadri, Annalisa Saltari, Carlo Pincelli

Laboratory of Cutaneous Biology, Department of Surgical, Medical, Dental and Morphological Sciences, University of Modena and Reggio Emilia, Modena, Italy

*Corresponding author:*

Alessandra Marconi

Laboratory of Cutaneous Biology, Department of Surgical, Medical, Dental and Morphological Sciences, University of Modena and Reggio Emilia

Via Del Pozzo 71

41124 Modena, Italy

Tel +39 059 4222812 Fax +39 059 4224271

e-mail: [alessandra.marconi@unimore.it](mailto:alessandra.marconi@unimore.it)

Number of word: ~~41494~~500

Number of references: ~~96~~106

Number of display: 4

Style Definition: Normal: Font: (Default) Times New Roman, Italian (Italy)

Style Definition: Balloon Text: Font: Italian (Italy)

Style Definition: Normal (Web): Font:

Style Definition: Byline

Style Definition: Titolo1

Style Definition: desc

Style Definition: details

Style Definition: Titolo2

Formatted: Font:

Formatted: English (U.S.)

Formatted: Font:

Formatted: Font:

Formatted: Font:

Formatted: English (U.S.)

Formatted: Font: English (U.S.)

Formatted: Font: English (U.S.)

For Review Only

**ABSTRACT**

Melanoma is one of the most studied neoplasia, although laboratory techniques used for investigating this tumor are not fully reliable. Animal models may not predict the human response due to differences in skin physiology and immunity. In addition, international guidelines recommend to develop processes that contribute to the reduction, refinement and replacement of animals for experiments (3Rs). Adherent cell culture has been widely used for the study of melanoma to obtain important information regarding melanoma biology.

Nonetheless, these cells grow in adhesion on the culture substrate which differs considerably from the situation in vivo. Melanoma grows in a 3D spatial conformation where cells are subjected to a heterogeneous exposure to oxygen and nutrient. In addition, cell-cell and cell-matrix interaction play a crucial role in the pathobiology of the tumor as well as in the response to therapeutic agents. To better study melanoma new techniques, including spherical models, tumorspheres, and melanoma skin equivalents have been developed. These 3D

Formatted: Font:

1  
2  
3  
4  
5  
6  
7  
8  
9  
10  
11  
12  
13  
14  
15  
16  
17  
18  
19  
20  
21  
22  
23  
24  
25  
26  
27  
28  
29  
30  
31  
32  
33  
34  
35  
36  
37  
38  
39  
40  
41  
42  
43  
44  
45  
46  
47  
48  
49  
50  
51  
52  
53  
54  
55  
56  
57  
58  
59  
60

models allow to study tumors in a microenvironment that is more close to the in vivo situation, and are less expensive and time consuming than animal studies. This review will also describe the new technologies applied to skin reconstructs such as organ-on-a-chip that allows skin perfusion through microfluidic platforms. ~~Although 3D in vitro models still need to be implemented, we expect to achieve a model morphologically, based on the new technologies, are becoming dynamically similar to normal and diseased skin~~ more sophisticated, representing at a great extent the in the near future, with vivo situation, the "perfect" model that will allow less involvement of animals up to their complete replacement, is still far from being achieved.

Formatted: Pattern: Clear

Formatted: Pattern: Clear

Formatted: Pattern: Clear

Formatted: Font: English (U.S.)

**KEYWORDS**

Melanoma, 3D models, spheroids, skin equivalent, skin-on-a-chip

Formatted: Font: English (U.S.)

For Review Only

## 1. INTRODUCTION

Formatted: English (U.S.)

Malignant melanoma (MM) is a highly aggressive cancer of the skin originating from melanocytes. MM is the most life-threatening tumor of the skin (70%), although melanomait represents only 4% of all skin cancers <sup>[1]</sup>. MM is regarded as a major health problem due to the high mortality associated with tumor and to its growing incidence. According to the World Health Organization, 132,000 melanoma skin cancers occur globally each year. The metastatic stage represents the major therapeutic challenge, as responders to conventional chemotherapy are still below 20% for mono- and below 30% for poly-chemotherapy <sup>[2]</sup>.

Formatted: English (U.S.)

Formatted: English (U.S.)

Melanoma is a heterogeneous disease, which suggests a richly complex etiology. Deep molecular analyses have revealed consistent genetic patterns among different melanoma subtypes. The latest estimate of mutation burdens is of ~17 mutations per Mb calculated by TCGA from whole-exome sequencing (WES) of 318 primary and metastatic melanomas originating from non-glabrous (hair-bearing) skin <sup>[3]</sup>. In melanoma, it was possible to isolate single cells of BRAF V600E/wt-NRAS and wt-BRAF/NRASQ16R genotypes from the same lesion <sup>[4]</sup>. In other studies, melanomas express heterogeneously tumor-associated antigens such as gp100 and melanoma antigen recognized by T cells-1 (MART-1) <sup>[5]</sup>. Cells not expressing MART-1 and gp100 escape immune surveillance, which may explain past failures in passive and active immunotherapies <sup>[6]</sup>. Future efforts will need to focus on targeting multiple coexistent aberrations in different pathways and addressing the mechanisms that underlie the tumor's propensity for growth and chemoresistance <sup>[7]</sup>. This in turn will lead to a rational basis for combinations of targeted treatments aimed at circumventing mechanisms of resistance to yield a clinical benefit. To these purposes, there is an evident need of tools that allow a better understanding of the pathomechanisms involved in melanoma. Moreover, it will be of paramount importance to develop new tools to evaluate the efficacy of novel therapeutic strategies.

Formatted: Font: English (U.S.)

1  
2  
3  
4  
5  
6  
7 Currently, different animal models are used to study melanoma development and to assess  
8 efficacy and safety of drugs in preclinical phase. Human tumor xenografts of established  
9 human melanoma cell lines or primary melanoma cells implanted subcutaneously and  
10 intradermally into immunosuppressed mice, allow the study of primary tumors and metastases

11  
12  
13  
14 <sup>[8]</sup>. Metastatic melanoma cell lines or primary tumor cells, ~~also injected into the mice tail vein<sup>[9]</sup>;~~  
15 ~~spontaneously metastasize to distant sites, such as the lung. Alternatively, tumor cells are~~  
16 ~~injected into the mice tail vein<sup>[9]</sup>;~~ injected into the mice tail vein<sup>[9]</sup>, spontaneously metastasize.  
17  
18  
19 However, established cell lines become inexorably altered in the process, thereby limiting their  
20 ability to predict clinical outcome and drug activity. Recently, the use of primary melanoma  
21 cells rather than established melanoma cell lines has become a standard for xenografting<sup>[8]</sup>.

22  
23  
24  
25  
26 The subcutaneous transplants of fresh tumor tissue into immunocompromised mice, the  
27 patient-derived xenograft (PDX) models<sup>[10]</sup> generates avatars of a melanoma patient who has  
28 relapsed on a drug. This way, 'mini human-in-mouse trials' or 'co-clinical trials' can be  
29 conducted for the selection of effective drugs and dosing regimen for that specific patient<sup>[8,10]</sup>.

30  
31  
32  
33  
34 Recently, using the the melanoma patient-derived orthotopic xenografts (PDOX) model to  
35 identify efficacious approved agents and experimental drugs, resected melanoma tissues were  
36 transplanted into the chest wall of nude mice to mimic the site from which they were taken  
37 from the patient<sup>[11]</sup>. However, as with all model systems, the PDXs have limitations, most  
38 notably the required use of immunocompromised mice. For simulating the natural progression

39  
40  
41  
42  
43 of melanoma as it occurs in humans, mouse models that involve the induction of  
44 carcinogenesis through multistage UVR or chemical agent treatments are also extensively used

45  
46  
47 <sup>[10,11,12,13]</sup>. More recently, genetically engineered mouse models have been exploited to study the  
48 effect of genetic alterations in melanoma initiation, progression, and metastasis <sup>[12,14]</sup>. Moreover,  
49 with the advancement of next-generation sequencing technology new mutations are being  
50 identified and new engineered models will be developed. Given that cancer is the product of

51  
52  
53  
54  
55  
56  
57  
58  
59  
60

1  
2  
3  
4  
5  
6  
7 complex interactions between the genotype and environment, the combined use of chemical  
8 carcinogen and genetically engineered models (GEM) is a logical approach to unravel the  
9 complex interplay between genetic susceptibility and environmental exposure. The clearest  
10 example of this is the increased spectrum of tumors observed in some GEM following exposure  
11 to carcinogens or radiation <sup>[14],13]</sup>. Less popular rodent models in melanoma research, i.e., Syrian  
12 golden hamsters and Mongolian gerbils are used for spontaneously occurring melanoma and  
13 for chemically-induced melanoma respectively <sup>[15]</sup>. In particular, Syrian hamster, the Bomirski  
14 melanomas, consists of 5 transplantable in vivo-variants and represent a good animal model  
15 for developing and testing potential melanoma vaccines <sup>[16]</sup>. In addition, an important feature  
16 of the Syrian hamsters is the variability in hair-coat coloration phenotypes, with numerous  
17 color mutants, which makes them particularly interesting objects of genetic studies and studies  
18 on the influence of hair color phenotypes on melanoma development <sup>[17]</sup>. Zebrafish model  
19 represents an alternative xenotransplant model *in vivo* that offers a rapid, efficient approach  
20 for assessing drug effects on human cancer cells at various stages of tumorigenesis <sup>[13,18]</sup>.  
21 Zebrafish embryos are particularly useful for microscopic analysis as they are translucent, thus  
22 offering the opportunity to visualize the metastatic process at high resolution <sup>[14,19]</sup>.

Formatted: English (U.S.)

Formatted: English (U.S.)

Formatted: English (U.S.)

23  
24  
25  
26  
27  
28  
29  
30  
31  
32  
33  
34  
35  
36  
37 However, in most instances, animal models may not predict the human response due to  
38 differences in skin physiology and immunity <sup>[15,16,20,21]</sup>. International guidelines on the use of  
39 animals for regulatory purposes are also increasingly making recommendations to develop  
40 processes that contribute to the reduction, refinement and replacement of animals for  
41 experiments (3Rs) <sup>[17,22]</sup>. Many industries now highlight the 3Rs as part of their corporate social  
42 responsibility, while the academic science base new exciting technologies, including stem cell,  
43 3-dimensional (3D) tissue constructs, bioprinting and organ-on-chips are being developed.

Formatted: Font: English (U.S.)



The availability of such systems and the easy access to melanoma cells have led to the development of various 2D and 3D melanoma models *in vitro*, whereby many questions will likely be addressed, without the use of animals.

Formatted: Font: English (U.S.)

## 2. MELANOMA CELL CULTURES

Formatted: Font: English (U.S.)

*In vitro* adherent cell culture of human melanoma cells includes their isolation and growing as a monolayer on plastic or coated tissue plates. Most studies on melanoma cell biology and preliminary screening of toxicity and efficacy of potential therapeutic molecules are performed in monolayer cultures [18,19,23,24]. Although these methodologies are easy to perform and have been instrumental for advancing our understanding of tumor biology, in 2D cultures, cancer cells organize as a monolayer, as opposed to the 3D more physiological structure. Malignant transformation, primarily driven by genetic mutations in cells, is also accompanied by specific changes in cellular and extra-cellular mechanical properties, such as stiffness and adhesion [20]. Mechanobiological<sup>[25]</sup>. While new computational approaches have detected similarity between tumor and cell lines<sup>[26]</sup>, mechanobiological signaling in 2D culture systems still fail to mimic solid tumors. In particular, the mechanical regulation influencing tumor growth *in vivo* and some characteristics, such as for instance hypoxia inside the tumor mass, cannot be reproduced in 2D cultures. Monolayer cultures do not recapitulate many of the complex properties of the *in vivo* melanoma microenvironment. In particular, cell cultures cannot reproduce melanoma cell interactions with extracellular matrix (ECM) and cell-to-cell communications required to regulate polarity, proliferation, adhesion, survival and proteolytic cleavage of the microenvironment, responsible for tumor metastasis. Indeed, the composition and 3D structure of the ECM undergo a continuous remodeling during tumor progression [22,27]. In addition, different drug responses were observed for cells grown in 3D cultures, as compared with 2D monolayers [22,28]. Finally, cells cultured in 3D models are more resistant than

Formatted: English (U.S.)

2D cultures to anticancer drugs [23,2429,30]. For these reasons, the evolution of the 3D culture systems can bridge the gap between traditional 2D cultures and in vivo melanoma models.

Formatted: Font: English (U.S.)

### 3. MELANOMA 3D MODELS

Over the last ten years, numerous 3D melanoma models have been developed. Spheroids can be formed only by cancer cells (monoculture) or by combining cancer and stromal cells (co-culture). The so called tumorsphere, is being increasingly used as an in vitro assay to study melanoma cancer stem cells (CSC). Skin equivalent is an advanced 3D model, which allows to study melanocyte/keratinocyte interaction in an in vitro reconstitute epidermis. In the last few year, microfluidic culture devices or skin on a chip models have become available, and reproduce a dynamic skin reconstruct, more similar to the in vivo situation.

Formatted: English (U.S.)

Formatted: Font: English (U.S.)

The 3D culture models represent a breakthrough in cancer research and development of new anti-cancer therapeutic strategies, fulfilling the principle of the 3Rs with the final reduction of animal experiments.

Formatted: English (U.S.)

Formatted: Pattern: Clear (White)

#### 3.1 SPHERICAL MODELS

The multicellular tumor spheroid (MCTS) was first developed by Sutherland and co-workers in the early 70s [25,31]. MCTS are composed by tumor cells grown in particular conditions allowing the formation of sphere-like 3D structure.

Formatted: Font: Not Bold, Not Italic, Font color: Auto, Pattern: Clear

Formatted: Justified, Right: -0", Don't adjust space between Latin and Asian text

Formatted: English (U.S.)

Formatted: Font:

Formatted: Font: English (U.S.)

Formatted: English (U.S.)

Formatted: Font:

Formatted: Font: English (U.S.)

It is well known that spheroid models better simulate the growth and microenvironment conditions of the tumor in vivo. In particular, MCTS show critical physiologic parameters, including cell-cell adhesion, barriers to mass transport, extracellular matrix deposition, cell-matrix adhesion and, in some cases, a necrotic core surrounded by a viable layer of quiescent and/or proliferating cells [26,27,32,33]. Comparative studies have shown that numerous genes

Formatted: Font:

Formatted: Font:

Formatted: Font:

Formatted: Font: English (U.S.)

associated with cell survival, proliferation, differentiation and resistance to therapy are differentially expressed in cells grown as MCTS versus 2D cultures [28,29,30,34,35,36].

Formatted: Font: English (U.S.)

We previously demonstrated that in melanoma MCTS the expression level of several melanoma markers (CD271, HIF-1 $\alpha$ , ABCB5 and Oct4) observed in skin lesion and freshly isolated cells are maintained in spheroids derived from the same patients up to 168h [31,37].

Formatted: Font: English (U.S.)

Over the years, several approaches have been proposed for MCTS generation. They are divided in scaffold-free and scaffold-based systems (Fig. 1). In the scaffold-free system, formation of MCTS occurs when tumor cells are placed in an environment where cell-cell interactions dominate over cell-substrate interactions and spontaneously aggregate to form a spherical 3D structure [32,38]. This non-adherent condition can be recreated by several techniques. The most used approach is the liquid overlay method where tumor cells are seeded on culture plate previously coated with a thin layer of inert substrate, such as agar, agarose or polyHEMA [33,39].

Formatted: Font: English (U.S.)

Formatted: Font:

Formatted: Font: English (U.S.)

Formatted: Font:

Formatted: English (U.S.)

Formatted: Font:

Formatted: Font:

Formatted: Font:

Formatted: English (U.S.)

The liquid overlay method leads to reproducible formation of one single MCTS per well, homogenous in size which makes them ideal for high-throughput screening of new therapeutic agents [34,40]. We have validated the spheroid model by using melanoma cell lines (primary radial growth phase or vertical growth phase and metastasis) (Fig. 2). Melanoma cells cultured in 2D showed fail to show differences among cell lines. On the other hand, when cells are cultured as MCTS, well distinct morphologic features appear already at 24 hours (Fig. 2A). In addition, MCTS are able to reflect the *in vivo* behavior, as shown by the growth curve and pixel areas typical of their original tumor cell (Fig. 2B and 2C).

Formatted: Font:

Formatted: Font:

Formatted: Font:

Formatted: Font: English (U.S.)

Formatted: English (U.S.)

The "hanging drop" cell culture is an alternative method to generate MCTS. In this case, a drop of cells suspension is placed on the lid of an inverted petri dish, thus letting cells grow in suspension avoiding the plate surface (Fig. 1). This technique is useful to amplify cells in a 3D system, but it is necessary to transfer MCTS in another plate for further investigation.

Formatted: English (U.S.)

Spheroids can also be generated by a bioreactor (spinner flask or microgravity) or by a rotatory cell culture system, where cells are driven to self-aggregate under dynamic culture condition. These methods allow the production of a large quantities of MCTS but not uniform in size <sup>[35,3641,42]</sup> (Fig.1). Recently, the formation of MCTS by encapsulating tumor cells in a Calcium alginate based membranes (Fig. 1) was described. This approach allows the preparation of large quantities of MCTSs of a well-defined size, but seems to reduce oxygen, nutrients and contact between cells <sup>[37,3843,44]</sup>. However, an aqueous core enclosed by hydrogel shell without water-immiscible condition was recently developed to overcome this limitation <sup>[3945]</sup>.

MCTS can also be formed by using a synthetic cyclic RGD (Arg-Gly-Asp) peptide, called cyclo-RGDfK(TPP). The RDG-motif, present in several ECM proteins is responsible for binding to integrins, thus providing cell to cell and cell-to-matrix interaction <sup>[4046]</sup>. Akasov and co-workers were able to induce the cell self-assembly of both normal and tumor cells by adding the cyclic RGDfK and the cyclo-RGDfK(TTP) directly to the monolayer cultures obtaining spheroids that were homogenous in size and useful to evaluate the cytotoxic effect of antitumor drugs <sup>[4147]</sup>.

The scaffold-based method consists in the use of a porous 3D scaffold which physically supports cell aggregation, allowing the formation of MCTS with a controlled size. Several scaffolds have been developed <sup>[42,4348,49]</sup>, in particular, Gong et al. created an agarose-based scaffold consisting in a micropore scaffold adaptable to 6-24-well plates. This system allows the rapid cellular assembly of cells to MCTS and It is completely transparent, allowing to monitor the spheroids formation by optical microscope <sup>[4450]</sup>.

Several studies have demonstrated that spheroids more accurately mimic the drug sensitivity/resistence of cancer cells of the real tumor. For this reason, spheroids are widely used as a model for drug screening and development <sup>[45,3451,40]</sup>. Both melanoma cell lines and human primary and metastatic cells could be employed to form MCTS and used to test new anti-tumor drugs in a contest that better reflect the in vivo behaviour of the tumor than 2D

Formatted: English (U.S.)

Formatted: English (U.S.)

Formatted: English (U.S.)

Formatted: English (U.S.)

Formatted: English (U.S.)

Formatted: English (U.S.)

Formatted: Font: English (U.S.)

monolayer condition. In order to predict the efficacy of new therapies, several tests could be performed directly on MCTS, including MTT assay, the measure of spheroids area in pixel, the apoptotic assay and the live-died assay based on Calcein AM and PI staining. Since MCTS resemble the tumor in vivo, they are a good model for study the tumor pathobiology in vitro. All molecular methods can be applied to study cells from spheroids at the cellular, protein, RNA and DNA level. The use of MCTS have increased the understanding of the intricate cell-cell and cell-matrix interaction <sup>[4652]</sup>, hypoxia <sup>[4753]</sup> and tumor metabolism <sup>[4854]</sup>. MCTS are also reliable in the study tumor progression and invasion, as well as in the evaluation of drugs effects on cells migration. They overcome the limitation of the most used invasion assay, such as the cell culture wound closure assay and the transwell cell migration and invasion assay, which are not able to recapitulate the 3D invasion that occurs in vivo <sup>[4955]</sup>. Different matrices are used to recapitulate the natural tumor microenvironment and evaluate cell migration <sup>[50,51,52,56,57,58]</sup>. The so called "collagen invasion assay", in which spheroids are immersed in a type I collagen matrix, is the most used method to assess the invasive capacity of cells in MCTS. Figure 3 shows an example of this assay performed by using five melanoma cell lines of different origin. To quantify the invasive ability, it is possible to measure the spheroids area and the invasion area in pixel by ImageJ software, the factor shape, the percentage of fragmentation and the distance reached by cells, as reported in several studies <sup>[53,49,33,59,55,37]</sup>. It should be also noted that the presence of stromal cells would better recapitulate the tumor microenvironment. These cells release growth factors and ECM components that influence tumor cell growth and migratory ability. Immune cells, fibroblast and endothelial cells are frequently used in tumor cells co-cultures. They could be seeded both after the formation of cancer MCTS or together with tumor cells in non-adherent conditions. The formation of MCTS with endothelial cells for the study of angiogenesis is widely recognised <sup>[54,55,60,61]</sup>. In addition, Marrero and co-workers reported an innovative spheroid model made by HaCaT cells grown

Formatted: Font:

Formatted: Font: English (U.S.)

Formatted: Font:

Formatted: Font:

Formatted: Font: English (U.S.)

Formatted: Font:

Formatted: Font:

Formatted: English (U.S.)

by using the bioreactor system known as the High Aspect Ratio Vessel (HARVs) in a microgravity environment. The HaCaT cells formed spheroids which were used as a scaffold to support the growth of B16.F10 mouse melanoma cells <sup>[5662]</sup>.

### 3.2 TUMOROSPHERE

MCTS is an innovative 3D model useful to study tumor cells in a context that better mimic the tumor microenvironment, but it does not allow to isolate and expand specific tumor cell sub-population. Cancer stem cells (CSC) are a small cell sub-population within a tumor equipped with self-renewal capacity and responsible for tumor maintenance and growth <sup>[57,58,59,63,64,65]</sup>. A system to expand mammalian stem cells in a sphere-like in vitro model was first described by Singh and co-workers who isolated and characterized normal neural stem cells grown as free-floating spheres, called neurospheres <sup>[60,66]</sup>. In the last years, this spherical model was applied to the CSC isolation from wide range of solid tumors, including melanoma <sup>[61,62,63,64,3867,68,69,70,44]</sup>.

The sphere formation assay consists in culturing cells at low-density in a specific medium in low-adherent conditions, where single cell is able to give rise to non-adherent sphere by clonal expansion <sup>[65,69,71,66]</sup>. A number of CSC markers, including CD133 <sup>[66,72]</sup>, the ABC transporter (ATP-binding cassette) involved in drug efflux (ABCB5) <sup>[67,73]</sup>, CD20 <sup>[68,74]</sup>, CD24 <sup>[69,75]</sup>, CD271 <sup>[70,76]</sup> are preliminary used to sort and to enrich the population. Nevertheless, this assay presents several disadvantages and limitations, such as excessive sensitivity to the culture method used (i.e. media composition, volume, surface area, etc.). In addition, cell density could favor cell fusion and aggregation rather than clonal expansion, while more differentiated cells exhibit sphere-forming capacity. Thus, the standard technique to evaluate the presence of CSC remain the transplantation of few cells into immunocompromised mouse and the observation of the capacity of continuously forming tumors after several xenotransplant experiment. The in vitro

Formatted: English (U.S.)

Formatted: English (U.S.)

Formatted: Font:

Formatted: English (U.S.)

Formatted: Font:

Formatted: Font:

Formatted: Font:

Formatted: Font:

3D methods remain a surrogate CSC assay which allow to reliably obtain an enrichment of tumor sub-population of CSC [77,78].

Formatted: English (U.S.)

### 3.3 HUMAN SKIN EQUIVALENTS

Formatted: English (U.S.)

As mentioned before, the interactions between tumor cell, neighbouring normal cell and ECM are extremely important as they are responsible for the control of cell behaviour and tissue homeostasis [74,79]. Studies indicate that basic fibroblast growth factor (bFGF) appear to be important in the promotion of melanoma proliferation and invasion [72,80]. Cancer-associated fibroblasts (CAFs) are an activated sub-population of stromal fibroblasts that have acquired a modified phenotype. CAFs have a prominent role in cancer development from initiation, to primary and metastatic progression and in drug resistance [73,74,81,82]. Recently, Dror and colleagues demonstrated that melanoma cells communicate with fibroblasts via melanosomes at the early steps of development, resulting in CAF formation [75,83]. Although MCTS recapitulate the 3D structure of the tumor, they fail to reproduce the complex organization of the tissue in vivo. In fact, they do not comprise the epidermal and dermal component that may influence melanoma invasiveness and aggressiveness.

Formatted: English (U.S.)

Formatted: English (U.S.)

Human skin equivalent (HSE) is an advanced 3D models which consists of in vitro reconstructed skin from isolated primary human cutaneous cells (keratinocytes, melanocytes and fibroblast) and ECM components. After the formation of each compartments, the reconstructed skin is left at the air-liquid interface allowing keratinocyte differentiation and stratification [76,84]. Histologically, HSE architecture and composition closely resemble human skin [77,85,8,78,86]. HSE has been used as an alternative to animal testing for studies of skin barrier function, skin irritation, wound healing, ultraviolet light-induced damage, for the treatment of burns and other wounds [79,80,81,87,88,89]. Moreover, this 3D model can be effectively used to study cell-cell interactions and effects of the stromal environment in the regulation of melanogenesis.

Formatted: Font: English (U.S.)

Formatted: Font:

Formatted: Font:

Formatted: Font:

Formatted: Font:

Formatted: Font:

Formatted: Font:

<sup>[81,90]</sup> proliferation and differentiation of keratinocytes. Furthermore, they can easily be engineered with specific genetic alterations in either dermal or epidermal compartments.

Formatted: Font color: Text 1, Pattern: Clear (White)

Formatted: English (U.S.)

Formatted: Font: English (U.S.)

Formatted: Font:

Formatted: Font: English (U.S.)

Also tumor cells, including melanoma, could be incorporate into HSE, thus providing an excellent model to study the progression and invasion of the tumor, as well as an excellent system for pharmacological analyses, reducing time and cost usually associated to animal experiments <sup>[7785]</sup>. Several approaches have been described to generate melanoma skin

Formatted: Font:

Formatted: English (U.S.)

Formatted: English (U.S.)

equivalent (MSE) in vitro. These protocols were firstly developed to generate healthy HSE, and melanoma cells were seeded with keratinocytes on the reconstructed dermis (Fig. 4A). One approach consists in the use of human de-epidermized dermis (DED). Skin biopsy of a donor is deprived of the epidermal layer by overnight incubation in sodium chloride and digested with Dispase II to remove the basement membrane. DED is placed on a sterile stainless steel rings with a diameter of 6 mm in a 24 well tissue plate. Primary keratinocytes, fibroblasts and melanoma cells are seeded together on DED and grown submerged for 24 hours, followed by 5-20 days of culture at the air-liquid interface to allow keratinocyte differentiation and stratification <sup>[82-7891,86]</sup>.

Formatted: English (U.S.)

In the collagen-based approach, dermis is reconstructed starting by acellular solution, consisting of rat tail or bovine type I collagen, which are placed on a tissue culture insert. After its polymerization, a cellular solution, consisting of human fibroblast and collagen I, is seeded on it and left in submerged condition for 5 days allowing the contraction of the collagen. Subsequently, primary human keratinocytes and melanoma cells are seeded onto the dermis and left in submerged condition for 4-5 days and at air-liquid interface for 5 to 20 days <sup>[7280]</sup>.

Formatted: Font: English (U.S.)

Other authors have developed an organotypic skin-melanoma spheroids model where melanoma MCTS are incorporated in the dermal compartment instead of being seeded together with keratinocytes above the collagen-derived dermal equivalents. In this model, MCTS in the dermis closely resemble the in vivo cutaneous melanoma metastases, resulting in



1  
2  
3  
4  
5  
6  
7 a large dermal melanoma nest instead that unpredictable nests that results by the approaches  
8 described above <sup>[2]</sup>. Recently, a new fully humanized MSE have been developed by Hill and co-  
9 workers, by using an inert porous scaffold (Alvetex®, Reinnrvate Ltd, Reproc cell group)  
10 incorporated with human fibroblasts to generate the dermis. This system overcomes the use of  
11 collagen derived from bovine or rat tail which are not representative of the normal skin  
12 microenvironment. The scaffold allows the 3D growth of fibroblasts, which are stimulated to  
13 produce their own ECM constituents, forming a stable human-like dermal compartment. In  
14 addition, in this method, melanoma cells are seeded onto the dermal equivalent prior the  
15 incorporation of keratinocytes, placing them in their original microenvironment <sup>[8392]</sup>.

Formatted: Font: English (U.S.)

24 It has been established that melanoma cells in HSE show a striking similarity to the growth and  
25 invasion properties of the lesion from which they are taken. MM progression consists of two  
26 phases, the Radial Growth Phase (RGP), where melanoma cells proliferate horizontally in the  
27 epidermis, and of a Vertical Growth Phase (VGP), where the tumor is more aggressive, and cells  
28 proliferate vertically invading the dermis <sup>[93]</sup>. As shown in figure 4B, primary RGP cell lines

Formatted: Font:

33 (WM115), stained with S100, are localized in the epidermis, while SkMel28 cell lines, derived  
34 from a more aggressive primary tumor with vertical growth, are localized at the dermal-  
35 epidermal junction. For this reason, MSE are widely used as an invaluable tool for the  
36 investigation of melanoma progression and spreading <sup>[83,7292,80]</sup>, which could help to understand

Formatted: English (U.S.)

41 the intricate process that leads to switch from radial to vertical growth and the invasion into  
42 the underlying tissue. In particular, melanoma invasion can be easily quantified by measuring  
43 the distance in depth reached by cells in the dermis <sup>[7886]</sup>. Finally, it is possible to test the anti-  
44 migratory effect of different drugs.

Formatted: Font: English (U.S.)

49 MSE is an attractive preclinical testing tools for novel therapeutic approaches, which could be  
50 useful to test efficacy as well as the pharmaceutical penetration and absorption by topical or  
51 intravenous administration of different drug. Since MSE is composed by different cell

populations consisting of normal and tumor cells, it is also possible to test the toxicities of the

drug by evaluating the effect on the surrounding non-transformed cells <sup>[84,85,94,95]</sup>.

However, the environment of melanoma in patients is even more complex, comprising of more cell types, such as immune cells, endothelial cells and adipocytes. Some authors have

developed full thickness HSE, including the hypodermal components and Langerhans cells

forming a tri-layered structure which mimics the full spectrum of biological functions of the

real skin <sup>[86,87,96,97]</sup>. A more complex MSE could allow to study the impact of soluble factors or

cytokines released from tumor cells or surrounding cells on melanoma invasion, drug response

in a context that is more closed to in vivo.

Additive manufacturing allows creating a complex tissue layer by layer in a process called

"bioprinting" in which living cells, ECM components and biomaterials together with growth

factors are 3D- printed in an intermingled fashion mimicking nature <sup>[88,98]</sup>. The interest in

bioprinting has significantly grown within the scientific and medical communities due to several

key advantages over conventional 3D culture methods <sup>[89,99]</sup>. These include the capacity to

create realistic, geometrically-complex morphologies formed by viable cells, high throughput,

precise reproducibility, low cost and a limited need for specialized training. However, a

complete 3D bioprinted human skin featuring all cell types has not yet been developed. The

lack of vascular and lymphoid systems represents the principal drawback.

### 3.4 MELANOMA-ON-CHIPS

Various organ-on-chip models are under development to reconstruct in vitro complex

microenvironments and to overcome some of the organotypic culture limitations, such as

inefficient tissue perfusion. Microfluidic platform are devices where living cells can be cultured

and continuously infused in micrometer-sized chambers, allowing a controlled release of

Formatted: English (U.S.)

Formatted: English (U.S.)

Formatted: Font:

Formatted: Font:

Formatted: Font:

Formatted: English (U.S.)

Formatted: Font:

Formatted: Font:

Formatted: Font:

Formatted: Font:

Formatted: Font: English (U.S.)

Formatted: English (U.S.)

Formatted: English (U.S.)

Formatted: Font: English (U.S.)

Formatted: English (U.S.)

growth factors or nutrients <sup>[90100]</sup>. Integration of microfluidics and electrical sensing modality in 3D tumour microenvironment may provide a powerful platform to accurately and rapidly monitor the response of cancer cells to a series of drugs <sup>[91101]</sup>. In addition, the on-a-chip approach at small-scale makes this platform also considerably cost-effective for drug screening applications <sup>[92102]</sup>. Mori and co-workers in a perfusable skin equivalent model with vascular channels coated with endothelial cells were able to measure the cell density and distribution following perfusion and the amount of drug absorbed into the vascular channel <sup>[93103]</sup>. Abaci and co-workers using a skin-on-a-chip platform with a unique capability to recirculate the medium, demonstrated that the cancer drug, doxorubicin, may have direct toxic effects on keratinocyte proliferation and differentiation <sup>[94104]</sup>. Pandya and co-workers using a microfluidic platform with multiple chambers and perfusion channels were able to delineate the drug susceptible and tolerant/resistant cancer cells in less than 12 hours <sup>[95105]</sup>. In addition, the implementation of nanotechnology-based microfluidics has given the possibility to explore cell interactions on a microscale level such as those occurring within a tumour immune-environment <sup>[96106]</sup>. A simple microfluidic structure (cell-on-chip), where both melanoma and immune cells could mutually migrate through the whole system, revealed that the mutual interactions between splenocytes and melanoma cells were markedly different depending on the nature of the spleen cells. In details, splenocytes appeared to possess markedly different migratory abilities when co-loaded with melanoma cells. On the other hand, melanoma cells displayed greater propensity to invade the microchannels in the presence of interferon regulatory factor 8 (IRF-8) KO splenocytes rather than when co-cultured with WT cells <sup>[96106]</sup>. Although it is necessary to develop and validate further platforms with reproducible tissue function levels, the ongoing models demonstrate a great potential to study healthy and diseased skin. Future improvements in biomaterials and microfluidic approaches are expected to obtain a reproducibility and efficiency of complex human tumour skin models including

Formatted: English (U.S.)

Formatted: English (U.S.)

various skin components and patient-specific cells. The optimization of microenvironment will facilitate the comprehension of the mechanisms underlying melanoma development and progression and, in addition to the integration of biomarkers/biosensors, the on-a-chip approach will revolutionize the drug screening and development, determining a more precise basis for providing personalized medicine.

Formatted: English (U.S.)

#### 4. CONCLUSIONS

Although 3D in vitro models are more and more efficient and sophisticated, they cannot fully replace the use of animals. They still need to be implemented to achieve a model that represents the in vivo situation in all its components morphologically and dynamically. ~~Given~~ Despite the ongoing progresses in technologies applied to 3D reconstructs, ~~we expect to have~~ the "perfect" model ~~in a very near future, with~~ that will allow less and less involvement of animals up to their complete replacement, is still far from being achieved.

Formatted: Font: English (U.S.)

#### Author contributions

AM, MQ, AS ~~Designed~~ designed the study; MQ, AS performed the research; AM, ~~MQ~~, AS, CP analyzed the data; AM, MQ, CP wrote the paper, MQ drew schematic representations. All authors have read and approved the final manuscript.

Formatted: Font:

Formatted: Font:

Formatted: Font: English (U.S.)

#### Conflict of interest

The authors declare no conflict of interest

1  
2  
3  
4  
5  
6  
7  
8  
9  
10  
11  
12  
13  
14  
15  
16  
17  
18  
19  
20  
21  
22  
23  
24  
25  
26  
27  
28  
29  
30  
31  
32  
33  
34  
35  
36  
37  
38  
39  
40  
41  
42  
43  
44  
45  
46  
47  
48  
49  
50  
51  
52  
53  
54  
55  
56  
57  
58  
59  
60

## REFERENCES

- [1] K. Klimkiewicz, K. Weglarczyk, G. Collet, M. Paprocka, A. Guichard, M. Sarna, A. Jozkowicz, J. Dulak, T. Sarna, C. Grillon, C. Kieda, *Cancer Lett.* 2017, 396, 10.
- [2] H. Vörsman, F. Groeber, H. Walles, S. Busch, S. Beisert, H. Walczak, D. Kulms, *Cell Death Dis.* 2013, 4, e719.
- [3] Cancer Genome Atlas Network, 2015, <https://cancergenome.nih.gov>
- [4] M. Sensi, G. Nicolini, C. Petti, I. Bersani, F. Lozupone, A. Molla, C. Vegetti, D. Nonaka, R. Mortarini, G. Parmiani, S. Fais, A. Anichini, *Oncogene* 2006, 25, 3357.
- [5] E.M. von Euw, M.M. Barrio, D. Furman, M. Bianchini, E.M. Levy, C. Yee, Y. Li, R. Wainstok, J. Mordoh, *J Transl Med.* 2007, 5, 19.
- [6] C.L.Jr. Slingluff, T.A. Colella, L. Thompson, D.D. Graham, J.C. Skipper, J. Caldwell, L. Brinckerhoff, D.J. Kittlesen, D.H. Deacon, C. Oei, et al., *Cancer Immunol Immunother.* 2000, 48, 661.
- [7] V.A. Nikolaou, A. J. Stratigos, K. T. Flaherty, H. Tsao, *J Invest Dermatol.* 2012, 132, 854.
- [8] K.A. Beaumont, N. Mohana-Kumaran, N.K. Haass, *Healthcare (Basel).* 2013, 2, 27.
- [9] C. Khanna, K. Hunter, *Carcinogenesis* 2005, 26, 3, 513.
- [10] G. Merlino, K. Flaherty, N. Acquavella, C.P. Day, A. Aplin, S. Holmen, S. Topalian, T. van Dyke, M. Herlyn, *M, Pigment Cell Melanoma Res.* 2013, 26, E8–E14.
- [11] R.M. Hoffman, *Int J Mol Sci.* 2017, 18, 1875.

Formatted: English (U.S.)

[10][12] S. R. Kelsall, B. Mintz, *Cancer Res.* 1998, 58, 4061.

[11][13] C.J. Kemp, *Cold Spring Harb Protoc.* 2015, 2015, 865.

Formatted: English (U.S.)

[12][14] J. Combest, P.J. Roberts, P.M. Dillon, K. Sandison, S.K. Hanna, C. Ross, S. Habibi, B. Zamboni, M. Müller, M. Brunner, N.E. Sharpless, W.C. Zamboni, *Oncologist.* 2012, 17, 1303.

Formatted: English (U.S.)

[15] M. Śniegocka, E.Podgórska, P.M. Płonka, M. Elas, B. Romanowska-Dixon, M. Szczygieł, M.A. Żmijewski, M. Cichorek, A. Markiewicz, A. A. Brożyna, et al., *Int. J. Mol. Sci.* 2018, 19, 1048.

Formatted: French (France)

[16] A. Slominski, R. Paus, *Int J Oncol.* 1993, 2, 221.

[17] P. Pour, J. Althoff, S.Z. Salmasi, K. Stepan, *J. Natl. Cancer Inst.* 1979, 63, 797.

[13][18] M. Haldi, C. Ton, W.L. Seng, P. McGrath, *Angiogenesis* 2006, 9, 139.

[14][19] K. Stoletov, V. Montel, R. D. Lester, S. L. Gonias, R. Klemke, *Proc Natl Acad Sci U S A.* 2007, 104, 17406.

Formatted: English (U.S.)

[15][20] J. Seok, H. S. Warren, A. G. Cuenca, M. N. Mindrinos, H. V. Baker, W. Xu, D. R. Richards, G. P. McDonald-Smith, H. Gao, L. Hennessy, C. et al., *Proc Natl Acad Sci U S A.* 2013, 110, 3507.

[16][21] I.W. Mak, N. Evaniew, M. Ghert, *Am J Transl Res.* 2014, 6, 114.

[17][22] M.L. Graham, M. J. Prescott, *Eur J Pharmacol.* 2015, 759, 19.

[18][23] H.A. Neumann, H.M. Runge, H.H.Fiebig, R. Engelhardt, G.W. Löhr GW, *J Cancer Res Clin Oncol.* 1986, 112, 165.

Formatted: English (U.S.)

[19][24] M.R. Carvalho, D. Lima, R.L. Reis, J.M. Oliveira, V.M. Correlo, *Stem Cell Rev.* 2017, 13, 347.

[20][25] S. Huang, D.E. Ingber, *Cancer Cell.* 2005, 8, 175.

Formatted: Font: 11 pt, English (U.S.)

Formatted: English (U.S.)

[26] F. Rambow, B. Job, V. Petit, F. Gesbert, V. Delmas, H. Seberg, G. Meurice, E. Van Otterloo, P. Dessen, C. Robert, et al., *Cell Rep.* 2015, 13, 840.

{21}[27] A. Malandrino, R.D. Kamm, E. Moeendarbary, ACS Biomater Sci Eng. 2018, 4, 294.

Formatted: Font: 11 pt

{22}[28] I. Serebriiskii, R. Castelló-Cros, A. Lamb, E.A. Golemis, E. Cukierman, Matrix Biol.

2008, 27, 573.

{23}[29] D. Loessner, K.S. Stok, M.P. Lutolf, D.W. Hutmacher, J.A. Clements, S.C. Rizzi,

Formatted: Font: 11 pt, English (U.S.)

Biomaterials. 2010, 31, 8494.

Formatted: Font: 11 pt

{24}[30] H. Karlsson, M. Fryknäs, R. Larsson, P. Nygren, Exp Cell Res. 2012, 318, 1577.

Formatted: Font: 11 pt, English (U.S.)

{25}[31] R.M Sutherland, J.A. McCredie, W.R Inch, J Natl Cancer Inst. 1971, 46, 113.

Formatted: English (U.S.)

{26}[32] R.Z Lin, H.Y. Chang, Biotechnol. J. 2008, 9, 1172.

Formatted: Font: 11 pt

{27}[33] L.A Kunz-Schughart, J.P. Freyer, F. Hofstaedter, R. Ebner, J. Biomol.

Formatted: English (U.S.)

Screen, 2004, 9, 273.

{28}[34] N.A. Cody, M. Zietarska, A. Filali-Mouhim, D.M. Provencher, A.M. Mes-

Formatted: English (U.S.)

Masson, P.N. Tonin, BMC Med. Genomics 2008, 1, 34.

{29}[35] T.T. Chang, M. Hughes-Fulford, Tissue Eng. Part A, 2009, 15, 55967.

{30}[36] M. Shimada, Y. Yamashita, S. Tanaka, K. Shirabe, K. Nakazawa, H. Ijima,

Formatted: Italian (Italy)

R. Sakiyama, J. Fukuda, K. Funatsu, K. Sugimachi. Hepatogastroenterology 2007,

54, 81420.

{31}[37] A. Saltari, F. Truzzi, M. Quadri, R. Lotti, E. Palazzo, G. Grisendi, N. Tiso, A. Marconi,

C. Pincelli, J. Invest. Dermatol. 2016, 136, 2049.

{32}[38] R.M. Sutherland, Science. 1988, 240, 177.

{33}[39] V. Dangles-Marie, M. Pocard, S. Richon, L.B. Weiswald; F. Assayag, P. Saulnier, J.G.

Juddle, J.L. Janneau, N. Auger, P. Validire, Cancer Res. 2007, 67, 398.

{34}[40] J. Friedrich, C. Seidel, R. Ebner, L.A. Kunz-Schughart. Nat Protoc 2009, 4, 309.

{35}[41] B.S. Youn, A.S. Sen, L. A. Behie, A. Girgis-Gabardo, J.A. Hassell, Biotechnol. Prog.

2006, 22, 801.

[36][42] Y. Fang and R.M Eglén, 3D Cell Culture, Drug Screening and Optimization. 2017, 22, 456.

Formatted: English (U.S.)

[37][43] S. Sakai, K. Inamoto, Y. Liu, S. Tanaka, S. Ariei, M. Taya, Cancer Sci. 2012, 103, 549.

[38][44] S. Zhang, C. Balch, M.W. Chan, H.C. Lai, D. Matei, J.M. Schilder, P.S. Yan, T.H. Huang, K.P. Nephew, Cancer Res, 2008, 68, 4311.

[39][45] K. Alessandri, B.R. Sarangi, V.V. Gutchenkov, B. Shina, T.R. Kieβling, L. Fetler, F. Rico, S. Scheuring, C. Lamaze, A. Simon et al., Proc Natl Acad Sci USA 2013, 110, 14843.

Formatted: English (U.K.)

[40][46] S. Kellouche, J. Fernandes, J. Leroy-Dudal, O. Gallet, S. Dutoit, L. Poulain, F. Carreiras, Tumor Biol. 2010, 31, 129.

[41][47] R. Akasov, D. Zaytseva-Zotova, S. Burov, M. Leko, M. Dontenwill, M. Chipier, T. Vandamme, E. Markvicheva, Int. Journal of Pharmaceutics, 2016, 506, 1498.

[42][48] J. Yang, M. Goto, H. Iso, C.S. Cho, T. Akaike, Biomaterials 2002, 23, 471.

[43][49] E.T. Verjans, J. Doijen, W. Luyten, B. Landuyt, L. Schoofs, J Cell Physiol. 2018, 233, 2993.

Formatted: English (U.S.)

[44][50] X. Gong, C. Lin, J. Cheng, J. Su, H. Zhao, T. Liu, X. Wen, P. Zhao, PLOS ONE 2015, 10, 1371.

Formatted: English (U.S.)

[45][51] L.B. Weiswald, D. Bellet, V. Dangles-Marie, Neoplasia, 2015, 17, 1.

Formatted: English (U.S.)

[46][52] F. Hirschhaeuser, M. Heike, C. Dittfeld, J. West, W. Mueller-Klieser, L.A. Kunz-Schughart, J. of Biotechnology. 2010, 140, 3.

[47][53] A. Raza, H.E. Colley, E. Baggaley, I.V. Sazanovich, N.H. Green, J.A. Weinstein, S.W. Botchway, S. MacNeil, J.W. Haycock, Sci. Rep. 2017, 7, 10743.

Formatted: English (U.K.)

[48][54] L.A. Kunz-Schughart, J. Doetsh, W. Muller-Klieser, K. Groebe, Am J Physiol Cell Physiol 2000, 278, C765.

Formatted: English (U.S.)

[49][55] D.F Quail, J.T. Maciel, K. Rogers, L.M. Postovit, J. Biomol. Screen. 2012, 17, 1088.



[50][56] K.L. Sodek, M.J. Ringuette, T.J. Brown, *Int J Cancer* 2009, 124, 2060.

Formatted: English (U.S.)

[51][57] B. Gole, M.B. Duran Alonso, V. Dolenc, T. Lah, *Pathol. Oncol. Res.* 2009, 15, 711.

[52][58] S. Hauptmann, D. Budianto, C. Denkert, M. Kobel, L. Borsi, A. Siri. *Oncology*, 2003, 65, 174.

[53][59] O. De Wever, A. Hendrix, A. De Boeck, W. Westbroek, G. Brems, S. Emami, M. Sabbah, C. Gespach, M. Bracke, *Int. J. Dev. Biol.* 2010, 54, 887.

[54][60] O. Oudar, *Crit. Rev. Oncol. Hematol.* 2000, 36, 99.

[55][61] N.E. Timmins, S. Dietmair, L.K. Nielsen, *Angiogenesis*, 2004, 7, 97.

Formatted: English (U.S.)

[56][62] B. Marrero, J.L. Messina, R. Heller, *In Vitro Cell Dev Biol Anim.* 2009, 45, 523.

[57][63] T. Shatton, M.K. Frank, *J. Invest Dermatol.* 2010, 130, 1769.

[58][64] T. Reya, S. J. Morrison, M.F. Clarke, I.L. Weissman, *Nature* 2001, 414, 105.

Formatted: English (U.S.)

[59][65] J.T. Lee, M. Herlyn, *J Cell Physiol.* 2007, 213, 603.

[60][66] S.K. Singh, I.D. Clarke, T. Hide, P.B. Dirks. *Oncogene.* 2004, 23, 7267.

Formatted: English (U.S.)

[61][67] D. Ponti, A. Costa, N. Zaffaroni, G. Pratesi, G. Petrangolini, D. Coradini, S. Pilotti, M.A. Pierotti, M.G. Daidone, *Cancer Res.* 2005, 65, 5506.

[62][68] A. Eramo, F. Lotti, G. Sette, E. Pillozzi, M. Biffoni, A. Di Virgilio, C. Conticello, L. Ruco, C. Peschle, R. De Maria, *Cell Death. Differ.* 2008, 15, 504.

[63][69] A.T. Collins, P.A. Berry, C. Hyde, M.J. Stower, N.J. Maitland. *Cancer Res.* 2005, 65, 10946.

Formatted: English (U.S.)

[64][70] M. Perego, M. Tortoreto, G. Tragni, L. Mariani, P. Deho, A. Carbone, M. Santinami, R. Patuzzo, et al., *J. Invest. Dermatol.* 2010, 130, 1877.

[65][71] B.A Reynolds, S. Weiss. *Science*, 1992, 255, 1707.

Formatted: English (U.S.)

[66][72] E. Monzani, F. Facchetti, E. Galmozzi, E. Corsini, A. Benetti, C. Cavazzin, A. Gritti, A. Piccinini, D. Porro, M. Santinami, et al., *Eur. J. Cancer* 2007, 43, 935.

[67][73] T. Schatton, G.F. Murphy, N.Y. Frank, K. Yamaura, A.M. Waaga-Gasser, M. Gasser,

Formatted: English (U.S.)

Q. Zhan, S. Jordan, L.M. Duncan, C. Weishaupt et al., *Nature*, 2008, 451, 7176, 345.

[68][74] D. Fang, T. K. Nguyen, K. Leishear, R. Finko, A.N. Kulp, S. Hotz, P.A. Van

Belle, X. Xu, D.E. Elder, M. Herlyn, *Cancer Research*, 2005, 65, 20, 9328.

[69][75] J. Dou, M. Pan, P. Wen, Y. Li, Q. Tang, L. Chu, F. Zhao, C. Jiang, W. Hu, K.

Hu, N. Gu, *Cell. Mol. Immunol*, 2007, 4, 467.

[70][76] A.D Boiko, O.V. Razorenova, M. van De Rijn, S.M. Swetter, D.L. Johnson, D.P.

Formatted: English (U.K.)

Ly, P.D. Butler, G.P. Yang, B. Joshua, M.J. Kaplan, et al. *Nature* 2010, 466, 7302, 133.

[77] T. Schatton, G.F. Murphy, N.Y. Frank, K. Yamaura, A.M. Waaga-Gasser, M. Gasser, Q.

Zhan, S. Jordan, L.M. Duncan, C. Weishaupt et al., *Nature*, 2008, 451, 34.

[78] M.F. Clarke, J.E. Dick, P.B. Dirks, C.J. Eaves, C.H. Jamieson, D.L. Jones, J. Visvader, I.L.

Weissman, G.M. Wahl, *Cancer Res.* 2006, 66, 9339.

[74][79] K.S. Smalley, M. Lioni, M. Herlyn, *In vitro Cell Dev Biol Anim.* 2006, 42, 242.

[72][80] F. Meier, M. Nesbit, M-Y. Hsu, B. Martin, P. Van Belle, D.E. Elder, G. Schaumburg-

Formatted: English (U.S.)

Lever, C. Garbe, T. M. Walz, P. Donatien, T. M. Crombleholme, and M. Herlyn. *Am. J.*

*Pathol.* 2000, 156, 1.

[73][81] N.A. Bhowmick, E.G. Neilson, H.L. Moses, *Nature* 2004, 432, 332.

[74][82] P. Micke, A. Ostman, *Expert Opin Ther Targets.* 2005, 9, 1217.

Formatted: English (U.S.)

[75][83] S. Dror, L. Sander, H. Schwartz, D. Sheinboim, A. Barzilai, Y. Dishon, S. Apcher, T.

Formatted: English (U.S.)

Golan, S. Greenberger, I. Barshack et al., *Nat Cell Biol.* 2016, 18, 1006.

[76][84] H. Mertsching, M. Weimer, S. Kersen, H. Brunner. *GMS Krankenhhyg Interdiszip.*

2008, 3, Doc11.

[77][85] C.A. Brohem, L.B da Silva Cardeal, M. Tiago, M.S. Soengas, S.B. de Moraes

Formatted: Italian (Italy)

Barros, S.S. Maria-Engler, *Pigment Cell Melanoma Res.* 2011, 24, 30.

[78][86] P. Haridas, J.A. McGovern, S.D.L. McElwain, M.J. Simson, *PeerJ*, 2017, 5:e3754.

[79][87] M. Ponec, J. Kempenaar, J. Skin Pharmacol. 1995, 8, 499.

[80][88] K. Jansson, G. Kratz, A. Haegerstrand, In Vitro Cell Dev. Biol. Anim.

1996, 32, 53440.

Formatted: English (U.S.)

[81][89] K. Nakazawa, H. Nakazawa, F. Sahuc, A. Lepavec, C. Collombel, O. Damour,

Pigment Cell Res, 1997, 10, 38290.

Formatted: English (U.S.)

[90] [A. Slominski, D.J. Tobin, S. Shibahara, J. Wortsman, Physiol Rev. 2004, 84, 1155.](#)

[82][91] R.A. Dawson, Z. Upton, J. Malda, D.G. Harkin, Transplantation 2006, 81, 1668.

[83][92] D.S Hill, N.D.P Robinson, M.P. Caley, M. Chen, E.A. O'Toole, J.L. Armstrong. S.

Przyborski and P. E. Lovat, Mol Cancer Ther. 2015, 14, 2665.

Formatted: English (U.S.)

[93] [JrW.H. Clark, D.E. Elder, D.I.V. Guerry, M.N. Epstein, M.H. Greene, M. Van Horn, Hum](#)

[Pathol 1984, 15, 1147.](#)

[84][94] J. Tsai, J.T. Lee, W. Wang, J. Zhang, H. Cho, S. Mamo, R. Bremer, S.

Gillette, J. Kong, N. K. Haass, et al., Proc. Natl. Acad. Sci. USA 2008, 105, 3041.

[85][95] J.T. Lee, L. Li, P.A. Brafford, M. van den Eijnden, M.B. Halloran, K.

Sproesser, N.K. Haass, K.S. Smalley, J. Tsai, G. Bollang, et al., Pigment Cell

Melanoma Res. 2010, 23, 820.

[86][96] E. Bellas, M. Seiberg, J. Garlick, D.L. Kaplan, Macromol. Biosci. 2012, 12, 1627.

[87][97] I.J. Kosten, S.W. Spiekstra, T.D. de Gruijl, S. Gibbs, Toxicol. Appl. Pharmacol. 2015,

287, 35.

Formatted: Italian (Italy)

[88][98] N. Cubo, M. Garcia, J.F. Del Cañizo, D. Velasco, J.L. Jorcano, Biofabrication. 2016,

9, 015006.

[89][99] H. Cui, M. Nowicki, J.P. Fisher, L.G. Zhang, Adv Healthc Mater. 2017, 6(1).

Formatted: English (U.S.)

[90][100] S.N Bhatia, D.E. Ingber, Nat. Biotechnol. 2014, 32, 760.

[91][101] A. Pavesi, G. Adriani, A. Tay, M.E. Warkiani, W.H. Yeap, S.C. Wong, R.D. Kamm,

Sci Rep. 2016, 24, 6, 26584.

[92][102] H.E. Abaci, Z. Guo, Y. Doucet, J. Jacków, A. Christiano, *Exp Biol Med* (Maywood).  
2017, 242, 1657.

Formatted: English (U.S.)

[93][103] N. Mori, Y. Morimoto, S. Takeuchi, *Biomaterials* 2017, 116, 48.

[94][104] H.E. Abaci, K. Gledhill, Z. Guo, A.M. Christiano, M.L. Shuler, *Lab Chip*. 2015, 15,  
882.

Formatted: English (U.S.)

[95][105] H.J. Pandya, K. Dhingra, D. Prabhakar, V. Chandrasekar, S.K Natarajan, A.S Vasan,  
A. Kulkarni, H. Shafiee, *Biosens Bioelectron*. 2017, 94, 632.

[96][106] F. Mattei, G. Schiavoni, A. De Ninno, V. Lucarini, P. Sestili, A. Sistigu, A. Fragale,  
M. Sanchez, M. Spada, A. Gerardino et al., *J Immunotoxicol*. 2014, 11, 337.

Formatted: English (U.S.), Pattern: Clear

Formatted: details, Left, Line spacing: single

Review Only

1  
2  
3  
4  
5  
6  
7  
8  
9  
10  
11  
12  
13  
14  
15  
16  
17  
18  
19  
20  
21  
22  
23  
24  
25  
26  
27  
28  
29  
30  
31  
32  
33  
34  
35  
36  
37  
38  
39  
40  
41  
42  
43  
44  
45  
46  
47  
48  
49  
50  
51  
52  
53  
54  
55  
56  
57  
58  
59  
60

## FIGURE LEGENDS

**Figure 1. Schematic representation of the several approaches to generate multicellular tumor spheroids**

Formatted: English (U.S.)

Formatted: Font: English (U.S.)

**Figure 2. Evaluation of proliferative capacity of five melanoma cell lines comparing 2D and 3D models.** Five melanoma cell lines of different origin were analyzed: WM115 and WM266-4,

Formatted: English (U.S.)

derived respectively from primary radial growth phase (RGP) and metastatic tumor from the same patient; SKMEL28, primary vertical growth phase (VGP) tumor; WM793B and 1205Lu, primary RGP and metastatic tumor derived from the same patient. (A) Cells were cultured as 2D cultures (upper) or by using the liquid overlay method (lower) and pictures of 3D spheroids were taken at different time points. (B) The proliferative capacity of cells cultured in 2D and in 3D was evaluated by MTT assay. (C, D) Pixel analysis of the pictures was performed to calculate total area occupied by MCTS. Statistical analysis was performed using the Student's t-test. \*

$p < 0.05$ ; \*\*  $0.01 < p < 0.05$

Formatted: Font: English (U.S.)

**Figure 3. Collagen invasion assay.** (A) Cells were seeded on agar to form spheroids and, after 72h of culture, were transferred in a well coated with a solution of collagen I derived from rat tail. (B) MCTS in collagen I were followed up and photographed from 24 to 72 hours after implanting. (C) To calculate the factor shape and the percentage of fragmentation were used, respectively, the following formulas:  $(\text{perimeter})^2/4\pi \cdot (\text{area})$  and  $(\text{invasion area}/ \text{total area}) \cdot 100$ . (D-E) To quantify the invasive ability the spheroids area (D) and the invasion area (E) were measured by ImageJ software. (F) The average distance reached by invasive cells was analyzed by ImageJ software making four measurements of the distance from the edge of the MCTS in the four cardinal directions. Statistical analysis was performed using the Student's t-test. \*  $p < 0.05$ ; \*\*  $0.01 < p < 0.05$

Formatted: Font: English (U.S.)

**Figure 4. Melanoma skin equivalent.** (A) Schematic representation of the different approaches used to reconstruct MSE. (B) MSE obtained using WM115 (RGP) and SKMEL28 (VGP) cell lines, were paraffin-embedded after 6 days of emersion. Sections were stained with S100 antibody and DAB was used as cromogen. Scale bar = 100 $\mu\text{m}$ .

Formatted: Font:

1  
2  
3  
4  
5  
6  
7  
8  
9  
10  
11  
12  
13  
14  
15  
16  
17  
18  
19  
20  
21  
22  
23  
24  
25  
26  
27  
28  
29  
30  
31  
32  
33  
34  
35  
36  
37  
38  
39  
40  
41  
42  
43  
44  
45  
46  
47  
48  
49  
50  
51  
52  
53  
54  
55  
56  
57  
58  
59  
60

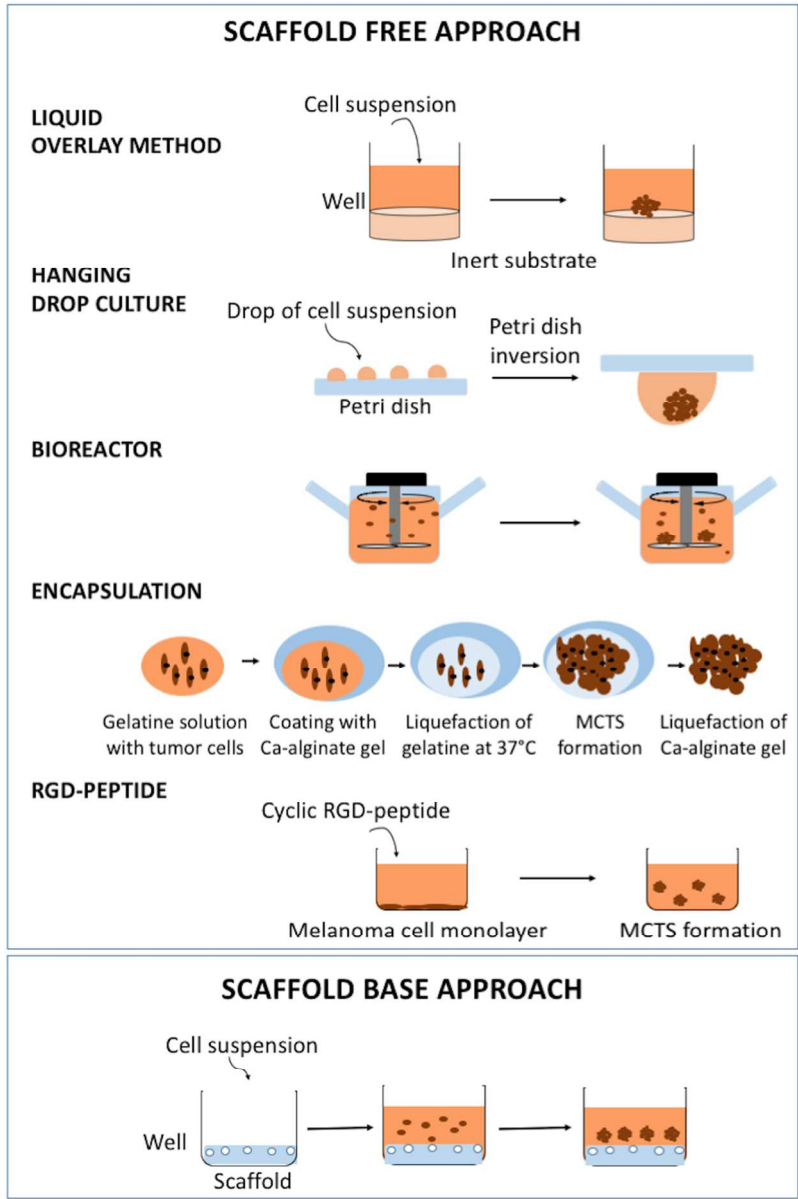


Figure 1. Schematic representation of the several approaches to generate multicellular tumor spheroids

81x121mm (300 x 300 DPI)

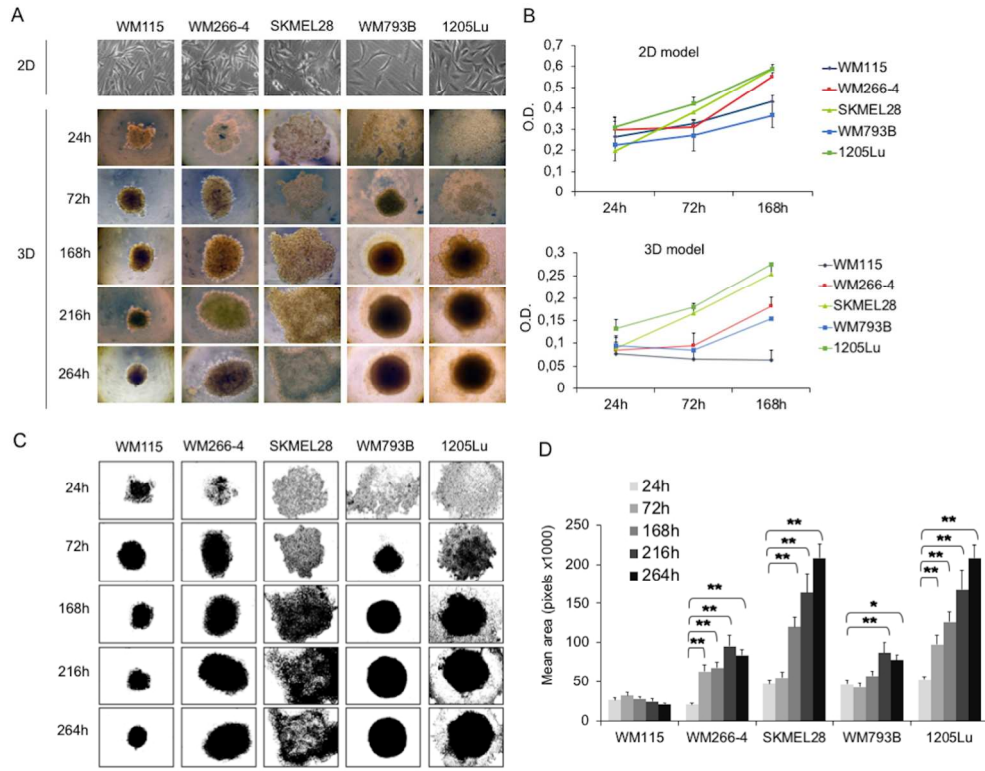


Figure 2. Evaluation of proliferative capacity of five melanoma cell lines comparing 2D and 3D models. Five melanoma cell lines of different origin were analyzed: WM115 and WM266-4, derived respectively from primary radial growth phase (RGP) and metastatic tumor from the same patient; SKMEL28, primary vertical growth phase (VGP) tumor; WM793B and 1205Lu, primary RGP and metastatic tumor derived from the same patient. (A) Cells were cultured as 2D cultures (upper) or by using the liquid overlay method (lower) and pictures of 3D spheroids were taken at different time points. (B) The proliferative capacity of cells cultured in 2D and in 3D was evaluated by MTT assay. (C, D) Pixel analysis of the pictures was performed to calculate total area occupied by MCTS. Statistical analysis was performed using the Student's t-test. \*  $p < 0.05$ ; \*\*  $0.01 < p < 0.05$

119x93mm (300 x 300 DPI)



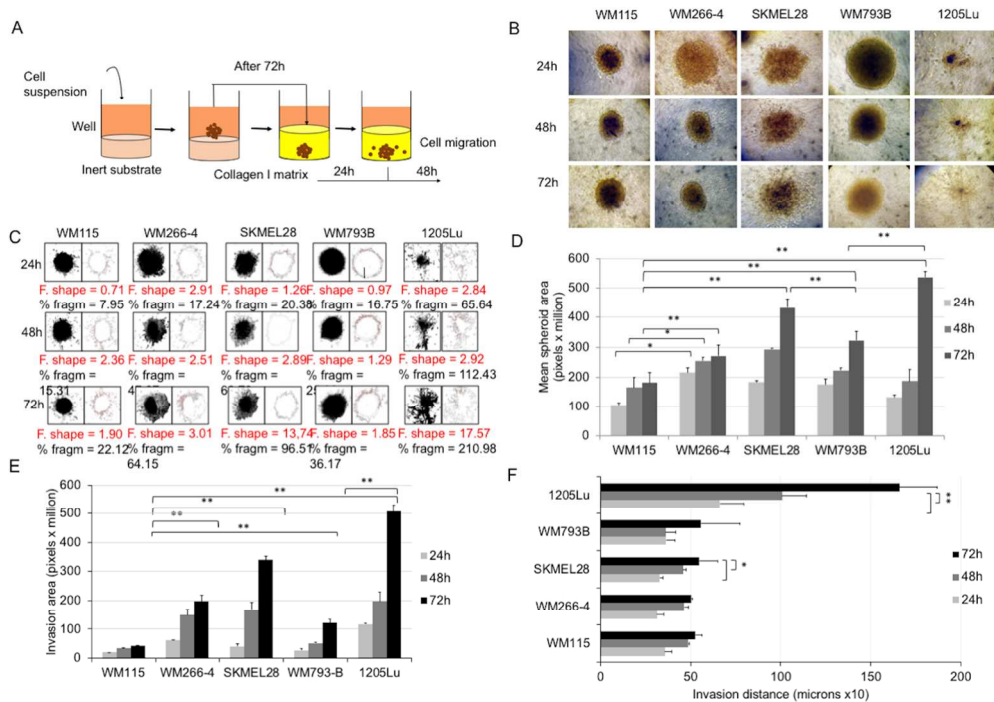


Figure 3. Collagen invasion assay. (A) Cells were seeded on agar to form spheroids and, after 72h of culture, were transferred in a well coated with a solution of collagen I derived from rat tail. (B) MCTS in collagen I were followed up and photographed from 24 to 72 hours after implanting. (C) To calculate the factor shape and the percentage of fragmentation were used, respectively, the following formulas:  $(\text{perimeter})^2/4\pi \cdot (\text{area})$  and  $(\text{invasion area}/ \text{total area}) \cdot 100$ . (D-E) To quantify the invasive ability the spheroids area (D) and the invasion area (E) were measured by ImageJ software. (F) The average distance reached by invasive cells was analyzed by ImageJ software making four measurements of the distance from the edge of the MCTS in the four cardinal directions. Statistical analysis was performed using the Student's t-test. \*  $p < 0.05$ ; \*\*  $0.01 < p < 0.05$

119x85mm (300 x 300 DPI)

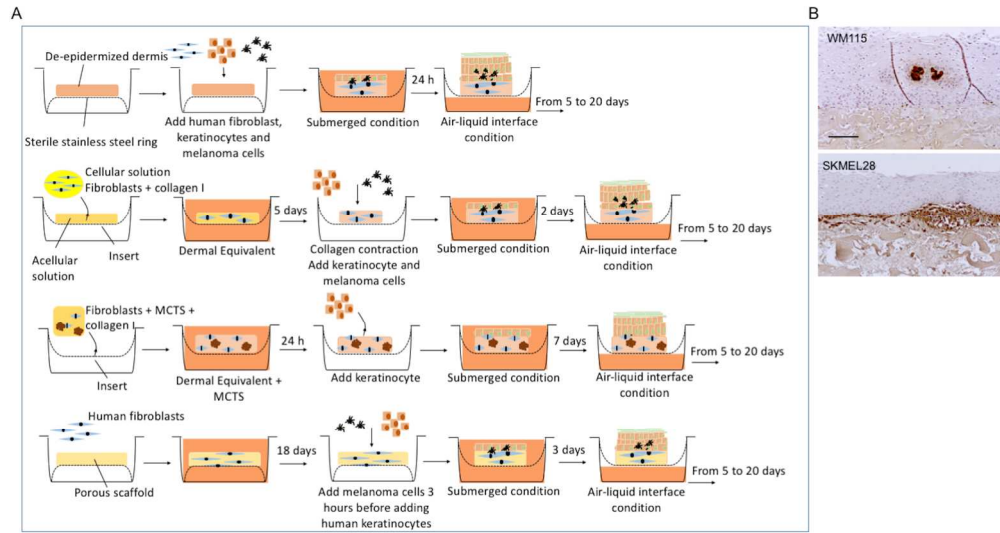


Figure 4. Melanoma skin equivalent. (A) Schematic representation of the different approaches used to reconstruct MSE. (B) MSE obtained using WM115 (RGP) and SKMEL28 (VGP) cell lines, were paraffin-embedded after 6 days of emersion. Sections were stained with S100 antibody and DAB was used as chromogen. Scale bar = 100 μm.

167x89mm (300 x 300 DPI)